Different sequential chemical treatments used to obtain bleached cellulose from orange bagasse

Paulo Henrique Fernandes Pereira (fernandes_eng@yahoo.com.br)
Sao Paulo State University Julio de Mesquita Filho: Universidade Estadual Paulista Julio de Mesquita Filho https://orcid.org/0000-0002-9741-2161

Luana Fernandes
UNESP: Universidade Estadual Paulista Julio de Mesquita Filho

Liziane Santos
UNESP: Universidade Estadual Paulista Julio de Mesquita Filho

Kelly Benini
USP: Universidade de Sao Paulo

Bárbara Pereira
USP: Universidade de Sao Paulo

Heitor Ornaghi Jr.
UCS: Universidade de Caxias do Sul

Maria Odila Cioffi
UNESP: Universidade Estadual Paulista Julio de Mesquita Filho

Research Article

Keywords: Orange bagasse, Chemical treatment, Lignocellulosic waste, Bleaching

Posted Date: June 10th, 2021

DOI: https://doi.org/10.21203/rs.3.rs-592178/v1

Different sequential chemical treatments used to obtain bleached cellulose from orange bagasse

Paulo Henrique F. Pereira[1]*, Luana L. Fernandes[1], Liziane B. Ubirajara Santos[1], Kelly C. C. de Carvalho Benini[2], Bárbara Pereira[2], Heitor L. Ornaghi Jr.[1], Maria Odila H. Cioffi[1]

[1]*Fatigue and Aeronautical Material Research Group, Department of Materials and technology, São Paulo State University (Unesp), School of Engineering, Guaratinguetá. 12516-410. São Paulo, Brazil*

[2]*Biocatalysis and Bioproducts Laboratory, Department of Biotechnology, Lorena School of Engineering, University of São Paulo, Lorena, São Paulo, 12602-810, Brazil*

[3]*Postgraduate Program in Engineering of Processes and Technologies (PGEPROTEC), University of Caxias do Sul (UCS), Caxias do Sul, 95070-560, Brazil*

**Corresponding author: fernandes_eng@yahoo.com.br*

Abstract

The development of efficient pretreatments is widely used in biobased products aiming to add value to the residue. In this study, orange bagasse is investigated for cellulose extraction under moderate chemical sequential extraction conditions. Three pretreatments are evaluated: alkaline treatment, organosolv, and residue insoluble alcohol. After, all pretreated samples are bleached. The results are analyzed by chemical composition, Fourier–transformed infrared spectroscopy, X-ray diffraction, and thermogravimetric analysis. In general, similar results are observed for all bleaching samples, independently of the pretreatment. It is observed a similar cellulose amount among the samples. When compared only to the pretreatments, alkaline shows to be a more effective way of presenting a higher crystallinity index. Hemicellulose and lignin are mostly removed after pretreatment. FTIR and XRD indicated that the pretreatment seems to be more effective in the first step. TG curves presented a more homogeneous pattern due to cellulose removal showing three steps for pre-treatment and two steps for bleached samples. The obtained cellulose has numerous potential applications, and a suitable route can be selected according to available reagents.

Keywords: Orange bagasse, Chemical treatment, Lignocellulosic waste, Bleaching

1. Introduction

Orange or sweet orange (Citrus sinensis L. Osbeck) is one of the 30 species of Citrus [1], and it is the most common cultivated fruit all over the world. It belongs to the Rutaceae family, being Brazil, the largest orange juice producer [2] in the world. An increase from 3.2 million metric tons in 2016/2017 to 50.2 million metric tons in 2020 is expected, mainly attributed to a substantial production in Brazil. Consequently, the number of underused by-products as peels, seeds, and bagasse (corresponding to around 50% of the total fruit) generated is enormous [3, 4]. These by-products can be used for animal feed, but most are disposed of in the environment without any type of treatment, offering a great diversity of low-cost raw materials as the production of bioethanol (a high value-added product). This is due to a very small portion of lignin presented besides high levels of polysaccharides. This combination becomes a single target for enzymatic hydrolysis, as described by Crypriano [5].

Most plant fibers are formed by a complex structure of crystalline cellulose microfibrils wrapped by an amorphous region consisting basically of lignin, hemicellulose, pectin, extractives, and waxes [6]. Bagasse orange contains peel (60–65%), internal tissues (30–35%), and seeds (0–10%), and it has high levels of soluble sugars, pectin, proteins, hemicellulose, and cellulose [7]. Thus, to convert these by-products into new value-added ones, different methods are available to separate specific components from the fibers, like cellulose isolation. The treatment methods can be classified as physic, chemical, physicochemical, biological/enzymatic, and combined [8]. The products obtained vary according to treatment [9].

Alkaline treatment is a chemical method, and it has high efficiency in removing amorphous/non-cellulosic components like lignin, hemicellulose, extractives, and waxes [10, 11]. However, this process also causes defibrillation of the components leaving the cellulose looser [12]. Organosolv is a promising approach for pretreatment of biomass since it can solubilize hemicellulose, lignin, and inorganic compounds as silica (SiO_2) found in plant cell walls [13, 14]. Moreover, compared to kraft or sulfite pulping methods, the reaction stages are less harmful to the environment [15]. Other advantages are: high-quality lignin obtained, value-added in the process, and solvent easily recovered by distillation, which leads to less water pollution.

Another example is the alcohol-insoluble residue (AIR), which is dependent on: i) type of starting material and, ii) type of analysis to be followed [16]. More intracellular/cytoplasmic material is found for coarsely ground or homogenized samples, becoming difficult the removal with subsequent aqueous or

65 solvent extractions. As an example, [17] describe a procedure that can be performed using small amounts
66 of fresh or dry material in microcentrifuge tubes. In the bleaching process, some oxidant agent such as
67 hydrogen peroxide (H_2O_2) or sodium chlorite ($NaClO_2$) is used to cause the oxidation and dissolution of
68 the lignin and hemicellulose remaining [18]. After bleaching, the fibers can be treated with a potassium
69 hydroxide solution to remove the residual hemicellulose and produce more pure cellulose fibers [19, 20].
70 Unlike acid or alkaline pretreatment, alkaline peroxide pretreatment can be performed at relatively milder
71 conditions (concentration, temperature) and atmospheric pressure while effectively removing lignin from
72 various agricultural residues.

73 Based on the literature above, this study has a significant contribution to the scientific field, a
74 profound understanding of three different chemical treatments regarding chemical composition, chemical
75 structure, crystallinity, and thermal behavior. The effect of hydrogen bond and hydrogen bond distance in
76 function after each treatment was evaluated by FTIR. A simulation of the thermogravimetric curve in the
77 function of chemical treatment was evaluated based on chemical composition, and crystallinity
78 parameters were also measured by XRD, aiming to corroborate the results and the morphology, using
79 scanning electron microscopy (SEM).
80

81 **2. Materials and Methods**

82 *2.1.1Reagents*

83 Orange bagasse (OB) from a local restaurant at Guaratinguetá city (São Paulo/Brazil) was used
84 as solid waste. Reagents employed were: sodium hydroxide (NaOH), acetic acid ($C_2H_4O_2$), hydrochloric
85 acid (HCl), ethanol (C_2H_5O), nitric acid (HNO_3), and hydrogen peroxide solution (H_2O_2 35 v/v), all
86 purchased from Vetec.

87 *2.1.2 Preparation of the orange bagasse (OB)*

88 OB was oven-dried at 60°C for 24h to remove all the moisture content. Afterward, OB was
89 chopped into smaller sizes using a cutter (GP 1500 AB) before milling into a fine powder with particle
90 size less than 35 mesh, using a basic knife grinder (WILLYE TE-650

91 *2.1.3 Chemical treatment of OB*

92 Three different chemical treatments were used: (*i*) alkaline treatment using NaOH, (*ii*)
93 organosolv with acetic acid, and (*iii*) AIR using ethanol. All treatments were bleached 1 and 2 times.

94 *Alkaline treatment (AT)*

After preparation, OB fibers were treated with 4% (w/v) alkaline solution of sodium hydroxide (NaOH) at fiber/solution ratio of 1:20 (g/mL) for 1 hour under constant stirring at 70° C. After, the solution was filtered until neutral pH, and the filtered is dried at 70 ° C until constant weight to obtain the alkaline treated (AT) fibers.

2.1.4 Bleaching Pulp (1B)

5g of dried AT fiber was used in an aqueous solution in 300 mL of an aqueous 4% (w/v) NaOH and 30 mL of 30% (v/v) H_2O_2 at 70 ºC, under mechanical stirring at 4000 rpm. After 1h of reaction, 50 mL of 4% (w/v) NaOH and 30 mL of 30% (v/v) H_2O_2 is added. The same procedure was repeated at each hour, up to three hours. After 3h of reaction, the fibers were vacuum filtered, water-rinsed, and the fiber washed with distilled water until pH ~7 and oven-dried at 60 ºC for 24 prior to obtaining 1B fibers.

2.1.5 Bleaching Pulp (2B)

To ensure further removal of the amorphous components, the procedure was repeated using 1B. 5g of dried 1B fibers were re-bleached using the same method with two hours of reaction; at each hour, 50 mL 4% (w/v) NaOH and 30 mL of 30% (v/v) H_2O_2 were added to the system. The fibers were vacuum filtered, washed with distilled water until pH~7, and finally oven-dried at 60 ºC until constant weight to obtain 2B fibers.

2.1.6 Bleached (2B/KOH)

Finally, 2B fibers were immersed in KOH 6% (w/v) in 1:20 ratio (w/v, fiber:solution) at 80 ºC with constant stirring (150 rpm) for 1h.

2.1.7 Organosolv Acetic Acid (OAc)

Acetosolv was conducted by the suspension of OB fibers in a flat bottom flask with reflux system with a mixture of solution (93% wt% acetic acid and 0.3% wt% HCl in distilled water at 110 ºC for 3 hours at 1:10 ratio (w/v, fiber: solution) [21]. After the reaction, the fibers were vacuum filtered, resulting in a lignin-rich black liquor; then, acetosolv pulp was washed with acetic acid 99.7% (wt%) at 80 ºC until the washed liquid is colorless. The fibers were water-rinsed to pH~7 and finally oven-dried at 50 ºC for 24 h, until constant weight. The sequence of bleaching treatments (Bleaching Pulp (1B), Bleaching Pulp (2B), Bleached (2B/KOH) was similar to those mentioned above.

2.1.8 Alcohol-insoluble residue (AIR)

Orange bagasse fibers were treated using 350 mL of ethanol in one of the balloons coupled to each of the glass tubes, 20g of milled orange bagasse fiber were added, the balloons were subjected to the

heating assembly, while a hose at the top carries cold water causing the vapor to be condensed nature passing through the fiber and removing the soluble residues in ethanol for 24h. After, the same sequence of bleaching treatments (Bleaching (1B), Bleaching (2B), and Bleached (2B/KOH) were followed, as described as mentioned above.

2.2 Characterization

2.2.1Chemical composition

Chemical composition of the OB (in nature), AT, AT_B, AC, AC_B, AIR, and AIR_B was carried out according to [22]. Acid-soluble lignin was determined according to (Dence 1992). Monomeric sugars are quantified by high-pressure liquid chromatography (Waters® HPLC) using an HPX-87H column (Bio-Rad). The temperature of the test was ~ 45 °C, and the samples were eluted with 5 mmol/L sulfuric acid at 0.6 mL/min.

2.2.2Fourier- transformed infrared (FTIR) spectroscopy (FTIR)

To evaluate the functional groups presented on the surface of the fibers, the ATR (Attenuated Total Reflection) technique was used. The spectra of fibers were determined in a Spectrum GX Perkin Elmer spectrophotometer by taking 8 scans in the range of 4000 to 400 cm^{-1} with a resolution of 4 cm^{-1}.

2.2.3 X-ray diffraction (XRD)

X-ray diffraction (XRD) pattern was measured on a Shimadzu diffractometer (XDR-6000 Model), operated at 40 kV and 30 mA with Cu K_α radiation (λ = 0.1542 nm), at angles of incidence of 10–50° (2θ/5 s). The crystallinity indices (CIs) were determined using the empirical Segal method (Segal et al., 1959), Eq. (1):

$$CI = \frac{I_{(200)} - I_{(am)}}{I_{(200)}} \times 100 \qquad (1)$$

Where: $I_{(200)}$ is the maximum intensity of the diffraction peak from the (200) plane at 2θ≈22°, and $I_{(am)}$ is the intensity of the minimum intensity between the major peaks. The values of *d*-spacing and the crystallite size perpendicular to the plane (*L*) for different crystalline planes also were calculated. The d-spacing of each plane was calculated using Bragg's equation, while the crystallite size was calculated by the Scherrer equation (2) (Ornaghi Jr. et al. 2014a) and the crystallite size was calculated using the Scherrer equation (Eq. (2)):

$$L = (0.94\lambda)/(H\cos\theta) \quad (2)$$

Where L is the crystallite size perpendicular to the plane, λ is the X-ray wavelength (0.1542 nm), H is the full-width at half-maximum in radians, and θ is the Bragg angle.

2.2.4 *Thermogravimetric analysis (TGA)*

Thermogravimetric curves (TG) were analyzed using TGA equipment (TG/DTG SII Nanotechnology Inc., Exstar TG/DTA 6200 model), were carried out at flow rate of 60 mL min^{-1}, using approximately 10 mg of each sample, at heating rates of 10 °C min^{-1} in N_2 atmosphere (0.05 L min^{-1}), in the temperature range from 25 to 660 °C.

3. Results and discussion

3.1 Chemical composition

According to NREL/TP-510 (Sluiter et al., 2012), the chemical composition estimated presents cellulose, hemicellulose, lignin, and ashes content for OB fiber and considering all chemical treatments.

Several pretreatments have been developed through the deconstruction of the cellulose-hemicellulose-lignin complex to facilitate the accessibility and the process of depolymerization of cellulose (Alvira et al. According to the chemical composition (Table 1), all chemical treatment followed by bleaching reached cellulose content greater than 75%, which demonstrates the efficiency of treatments in purifying cellulose. However, an increase in the percentage of lignin was observed after each treatment (AIR, AC, and AT), mainly caused by removing extractives.

Tab.1 *Influence of the chemical treatment on chemical composition of the tested fiber*

Fractions (%)	In natura	AIR	AIR_B	AC	AC_B	AT	AT_B
Ashes	6.2 ±0.1	6.6±0.04	3.07±0.04	3.06±0.03	2.1 ±0.02	6.2±0.02	2.92 ±0.03
Extractives	41.6±1.5	n.a*	n.a*	n.a*	n.a*	n.a*	n.a*
Lignin	5.1 ±0.1	7.86 ±0.04	2.00 ± 0.15	13.41±0.53	2.80±1.0	6.8 ±1.0	2.600 ±0.19
Cellulose	22.9 ±0.5	31.05±4.1	79.34±4.1	27.28 ±3.6	78.1±0.7	46.2±0.3	78.94±1.4
Hemicellulose	24.1±0.1	18.10±3.7	16.33±1.9	18.31±1.1	1.5±0.3	4.9±0.1	16.49±0.98
Total	99.9±2.5	63.64±3.8	100.7±6.1	62.061±1.8	79.6±2.1	64.1±2.6	100.9±2.1

*not analyzed

The removal of non-cellulosic components from biomasses can influence the properties of the material obtained after chemical treatments. Changes in chemical structures can be observed in the change of thermal behavior and crystallinity index of the materials compared to their respective raw materials.

3.2 FT-IR spectroscopy

FT-IR spectroscopy is a very useful technique for analyzing the structure of fiber components [24] and the chemical changes in fibers induced by different factors as chemical treatment [25], aging [26, 27], or microorganisms [26].

Figure 1 presents the FTIR spectra for all fibers studied. It is clear differences in absorption by bleached samples, independently of the chemical treatment. Aiming to help the reader visualize the results obtained, FTIR discussion was divided into two main regions [28] *i*) from 4000 cm^{-1} to 2700 cm^{-1} and *ii*) from 1900 cm^{-1} to 500 cm^{-1}. The former includes OH and CH stretching bands at 3400 cm^{-1} and 2900 cm^{-1}, respectively. The second is assigned to different stretching vibrations of other groups from cellulose, hemicellulose, and lignin in 1900-800 cm^{-1}. Besides, the OH region is particularly useful for elucidating hydrogen-patterns while CH stretching mode elucidates carbonyl stretching vibrations of the carboxyl and acetyl groups in hemicelluloses and alkenes stretching of the aromatic ring in lignin [29]. Hence, both regions were treated separately.

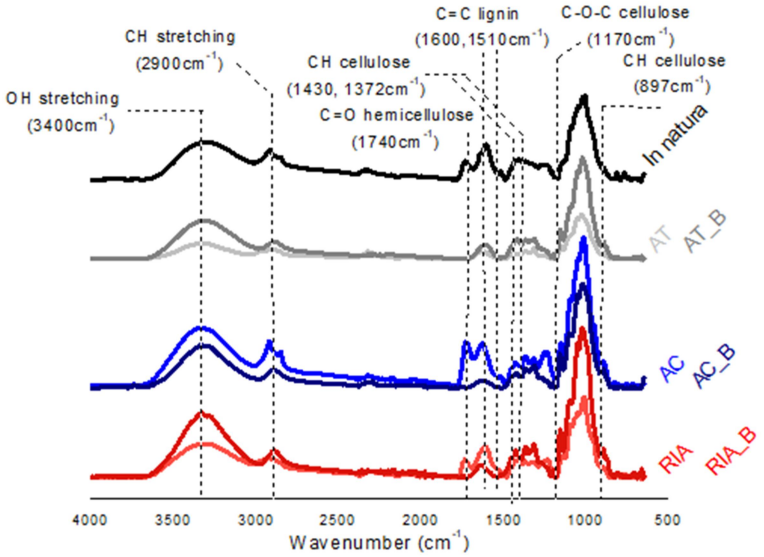

Fig. 1 *FTIR spectra for orange bagasse with the respective treatments*

Hydroxyl stretching absorption

Each hydroxyl group in fiber gives a single stretching band at a frequency that decreases with increasing hydrogen bonding strength [30]. The mixture of inter-and intramolecular hydrogen bonds is responsible for various properties of lignocellulosic materials. Also, it is responsible for the broadening of the OH band in the IR spectra. The chemical treatment can be responsible for changes in peak wavenumber [31].

Regarding the OH stretching region, the broad band from orange bagasse is from variations in the degree of hydrogen bonding between OH groups in the cellulose crystal/aggregated states, hemicellulose, lignin, and water [32]. With the removal of hemicellulose and lignin from chemical treatment, the relative increase of absorbance is taken as an indication of more organized cellulose. Consequently, sharper bands with the reduced band are expected due to the vibrations contribute at the same frequency. Thus, a reduction in overall area intensity in the OH region is observed in bleached, treated samples. As a consequence, higher-order suggests higher crystallinity (analyzed in section 3.3). In our study, sharper peaks are observed for bleached samples, but the width seems not to be altered.

A shift to a higher wavenumber is observed at the maximum absorbance for hydrogen-bonded in the case of all bleached fibers in the OH stretching region. This could be indicative of a decrease in the intramolecular hydrogen bonding. The values obtained for *in natura* 3298.68 cm^{-1}, AT: 3227.20 cm^{-1}, AT_B:331.41cm^{-1}, AC: 3327.58cm^{-1}, AC_B:3332.49cm^{-1}, AIR: 3307.17cm^{-1}, and AIR_B:3313.04cm^{-1}. When compared to *in natura* fiber, most of the fiber had higher maximum absorbance. Also, all peak shift for higher maximum for all bleached fibers. All bleaching processes increased the peak height-more organized structure. Consequently, the crystallinity index tends to increase. Using the values obtained, it is possible to estimate the energy of the hydrogen bonds (E_H) (Equation 3) and the hydrogen bonding distances (R) using the Sederholm equation (Equation 4):

$$E_H = \frac{1}{K}\left[\frac{\nu_0 - \nu}{\nu_0}\right] \quad (3)$$

$$\Delta\upsilon\ (cm^{-1}) = 4{,}43 * 10^3(2{,}84 - R) \quad (4)$$

where: $\Delta\upsilon = \nu_0 - \nu$, ν_0 is the monomeric OH stretching frequency, is taken to be 3560 cm^{-1} for the former and 3600 cm^{-1} for the latter, ν is the stretching frequency observed in the IR spectrum, and K is a constant = 262.5 kJ. Table 2 presents the calculation of FTIR parameters based on the Equations above.

Even with differences in maximum peaks described earlier, the hydrogen bond distance was not significantly altered by treatment. The energy of the overall OH bonds unexpectedly decreases after

bleaching. Maybe this can be attributed to a loss of overall OH bonds due to hemicellulose and lignin removal and not necessarily to the energy per se. Chemical composition showed that hemicellulose and lignin were drastically removed after respective treatment, so the loss of energy may correlate with it.

Tab. 2 *The effect of chemical treatment on the hydrogen bonding energy and hydrogen bond distance for OB fiber*

Samples	Hydrogen bonding energy (EH) (kJ.mol-1) *	Hydrogen bond distance (R) (Å) *
In natura	25.26	2.77
AT	30.40	2.75
AT_B	23.99	2.77
AC	23.19	2.78
AC_B	22.83	2.78
AIR	24.65	2.77
AIR_B	24.23	2.77

Since the OH region is composed of two intramolecular, one intermolecular, and one OH stretching [24], the results suggest that after treatment, there is a more intense disruption of the hydrogen bonds at the C-3 and C-6 position in the cellulose [33].

The band referred to the lignin phenolic group (3591/3579 cm-1 – absorbed water weakly bound and intramolecular hydrogen bond) was not observed for all bleached samples. The bands at 3438/3435 cm^{-1} are assigned to the O-H intermolecular hydrogen bonds involving the C6 position (primary hydroxyl groups). At 3348/3345 cm^{-1}, the frequencies are attributed to the O_5-H_5···O_3 intramolecular hydrogen bond.

If it is considered cellulose I_β and cellulose I_α (two crystalline allomorphs): at 3226/3217 cm^{-1}, O_6-H_6···O_3 intramolecular hydrogen bonds existing only in triclinic I_α cellulose; while the amount of monoclinic phase I_β is assigned at 3276 cm^{-1}. The results indicate that cellulose I_β is predominant even after chemical treatment.

CH stretching absorption

The spectrum is more complex in this region due to different stretching vibrations of the various groups from the main bagasse fiber components. The ranges in the 1800-800 cm^{-1} are presented in Figure 2. The following groups are attributed to lignin: C=C (1595 cm^{-1}), C-O stretching (1510 cm^{-1}), or

bending (1270 cm^{-1}). Other groups as C-H (1460 cm^{-1}), C-O deformation (1425 cm^{-1}), C-O bending (1335 cm^{-1}), or C-O stretching (1220 cm^{-1} and 1110 cm^{-1}) are assigned to different groups for lignin and carbohydrates. The bands at 1735, 1375, 1240, 1165, 1060, 1030 cm^{-1} are assigned to characteristic C=O, C-H, C-O-C, C-O deformation or stretching vibrations of different groups from carbohydrates. Due to the more significant number of cellulose groups presented, the bands assigned to cellulose are higher for pre-treatment than their respective bleached samples.

The presence of other remaining components is observed in the 1400-1750 cm^{-1} region. The presence of lignin, hemicelluloses (C=O stretching vibration of carboxyl and acetyl groups in xyloglucan), or pectin by the stretching vibration of C-O bond for esters at 1730 cm^{-1}. For NaOH samples, pectin should be discarded due to the acidic pre-treatment [34] and chemical composition. Also, the presence of this band is not observed. The bands at 1440-1600 cm^{-1} are assigned to the stretching vibration of lignin aromatic rings (Mariño et al., 2018a). However, the low intensity of the peaks corroborates the idea of detaching mainly cellulosic products from all samples. All bleached samples showed lower intensity about their pre-treatment.

FTIR spectroscopy can also offer a quantitative lignin determination in fiber. The intensity of the band of aromatic skeletal vibrations around 1510 cm^{-1} is a measure of the lignin content. Faix [35] indicates a non-linear equation which describes well the relation between the lignin content and the height of the 1510 cm^{-1} band (Equation 5):

$$\%\, lignin = -1.23 + 193.4.\, x - 279.8x^2 \qquad (5)$$

Where x is the band intensity determined by the baseline method.

The lignin content calculated in this study was possible to calculate only for in nature and RIA, and the results found were 31.84 % and 9.37%, respectively. The results are in good agreement with the chemical composition [36–39]. Faix considers that the calculus is valid only for lignin content from 5-30%. But the result obtained for *in natura* showed a good correlation with chemical composition, and it seems to be valid in this case. FTIR calculus so far illustrates that the mean spectra contained specific information that might be useful to distinguish bagasse fiber from most chemical treatments.

Relative crystallinity based on FTIR analysis

The total crystalline index (TCI) and the hydrogen bond intensity (HBI) were estimated based on literature [40]. TCI is proportional to the crystallinity degree and is calculated by the bands at 1372 cm^{-1} and 2900 cm^{-1} bands ratio, and it defines an empirical crystallinity index. HBI is regarded as the degree of

intermolecular regularity (crystallinity) and is calculated by the ratio between the absorbance bands at 3400 $cm^{-1,}$ and 1320 cm^{-1} is used to study the HBI of the OB fibers with different chemical treatments [41]. Since the structure of the species is the same, a comparable result among other treatments can be done [42].

Table 3 presents TCI and HBI calculated for all samples studied. TCI ratio in bleached samples ranged from 0.25 to 0.44. Regarding HBI, it ranged from 1.51 to 7.94. These values are in agreement with the IR ratios published elsewhere [42]. Since chemical treatment modified chemical composition, it is expected that the band at 897 cm^{-1} be stronger for cellulose II and amorphous cellulose. Cellulose I change to cellulose II depends on several factors; it can be cited chemical treatment, decrystallization, and changing the crystal polymorph [43].

Comparisons are made within each group of samples, given the small variation between the components. IR crystallinity is calculated from two measurements for each sample, and a mean ratio is after that calculated. An increase in IR crystallinity with treatment shows that for bleached treatments, there are effective changes in IR spectra. HBI results showed decreased hydrogen bond intensity with bleaching, maybe due to removing OH intramolecular bonds, hemicellulose, and lignin components.

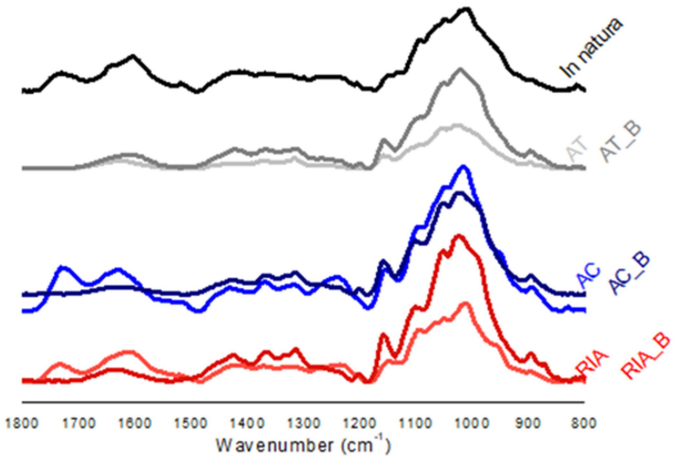

Fig. 2 *1800-800 cm-1 CH stretching absorption region for OB fiber and all chemical treatment*

Tab. 3 *Infrared crystallinity ratio and hydrogen bond intensity for the OB fibers after treatment*

Sample	IR crystallinity ratio	HBI A3400/A1320
In natura	0.26	1.36
AT	0.30	1.66
AT_B	0.42	1.55
AC	0.25	1.75
AC_B	0.34	1.52
AIR	0.25	1.31
AIR_B	0.44	1.55

3.3 X-ray diffraction (XRD)

X-ray diffraction patterns of the OB fiber with the respective treatments are shown in Figure 3. In general, two main crystalline peaks are found for all profiles. According to Segal, the crystallinity index was calculated using the main peak, referred to as the crystallographic plane (200) at ~22.3º 2θ reflection, and 18.5º 2θ reflection of the amorphous phase. All further parameters are calculated from the 200 crystallographic planes.

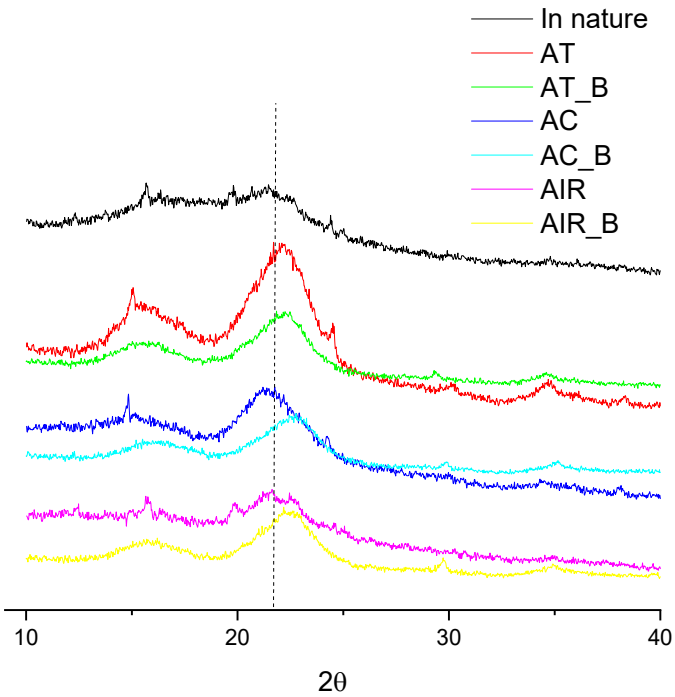

Fig. 3 *XRD curve for in natura, AT, AT_B, AC, AC_B, AIR and AIR_B samples. Dotted line is a guide for the eye representing 200 crystallographic planes*

Changes in the polymorphism of cellulose samples can be visually detected by evaluating the overall intensities of the diffraction peaks originating from the cellulose types and are dependent on

atomic coordinates and unit cell dimensions. Changes in crystal type and chain conformation are feasible and are dependent on solvent, additives, temperature, time, external pressure, among other factors [44]. Mansikkamaki et al.[45] studied the conversion from cellulose I to cellulose II in NaOH mercerization performed in alcohol-water systems X-ray diffraction. The authors developed a mathematical method to evaluate the conversion more exactly and survey the effects of different alkali treatments on cellulose crystals.

Table 4 shows the apparent lateral crystallites sizes (L) determined by the Scherrer equation and the apparent crystallinity degrees obtained by the Segal method for OB fibers. The result of OB is in agreement with the literature [34] and with values published elsewhere. The lowest crystallinity index was found *in natura* OB fiber. All treatments promoted an increase in the crystallinity index. All bleached treatments present similar results.

The results obtained from XRD differ from those obtained from FTIR, and no significant correlations could be established between both techniques, except for a general increase in the crystallinity index for bleached samples. But the parameters using FTIR must be used carefully and corroborated with other results. FTIR is sensitive to the polymer chain's chemical environment and XRD by the crystal lattice structure, so FTIR is an indirect method.

Tab. 4 *XRD parameters calculated from diffractograms*

Sample	L_{200}	FWHM (200)	Cr.I.(%)
In natura	5.22	1.62	15.1
AT	3.47	2.44	42.9
AT_B	3.81	2.22	49.0
AC	4.10	2.06	29.4
AC_B	3.47	2.44	48.3
AIR	3.30	2.56	22.8
AIR_B	3.59	2.36	52.0

The removal of hemicellulose and lignin increase the regularity of the crystal lattice due to a more organized structure is maintained in the compound, i.e., reduces the amorphous portion of the samples. Agarwal (2016) [46] studied hydrothermal treatment and compared it to its native state. The authors constated that cellulose becomes more consolidated and partly crystalline with treatment. The thermal treatment is responsible for the crystallization of organized aggregates. FTIR calculus uses regions where removing these components is more visible in some specific bands, being less precise concerning XRD results. The removal of less ordered carbohydrates presents a sharper FTIR peak,

indicative of a more organized structure, but the values calculated follow a certain trend but are less precise in comparison to XRD results.

According to [47], Segal Cr.I. depends on FWHM, crystallite size, and cellulose polymorph, while (Agarwal et al., 2016) (based on Raman spectroscopy) suggested that FHWM from XRD is a measure of the existing disorder in cellulose, which can be considered as the degree of lateral order (DOLO), related with to Cr. I. Changes in FHWM are related to change in crystal size and may involve changes in DOLO instead of crystallinity, as could be our case if it is assumed that the aggregated state of wood and holocellulose samples are not crystalline.

Regarding the lateral crystallite size (L), a close relationship with the XRD Cr.I. is not observed. The variations of these parameters could be attributed to the removal of lignin, hemicellulose, and less ordered carbohydrates, which could entail the degradation of small crystallites that increase the average lateral crystallite size. Our samples present lower values when compared to literature.

[48] suggested a co-crystallization of crystalline domains promoted by the removal of polysaccharides. In this case, the isolation via alkaline extraction mostly removes hemicellulose, low molecular weight, and disordered cellulose chains. Hence, the remaining fraction is mainly constituted of cellulose, and only traces of hemicellulose in the remaining solid are expected, as was confirmed by the reduction of 1740 cm^{-1} band intensity in FTIR and compositional analysis. As FTIR and XRD indicated, the treatment seems to be more effective in the first step. The alkali solution penetrates the more disordered or amorphous regions, whereby cellulose chains in the amorphous region rearrange into antiparallel cellulose II while the crystalline regions are hardly affected. As the swelling of cellulose continues, the mobility of the cellulose chains is enhanced; hence the crystalline cellulose gradually diminishes in size.

3.4 Thermogravimetric Analysis

The effect of each chemical treatment sequence on the thermal properties of orange bagasse fiber is analyzed based on Fig. 4 and 5, and Table 5.

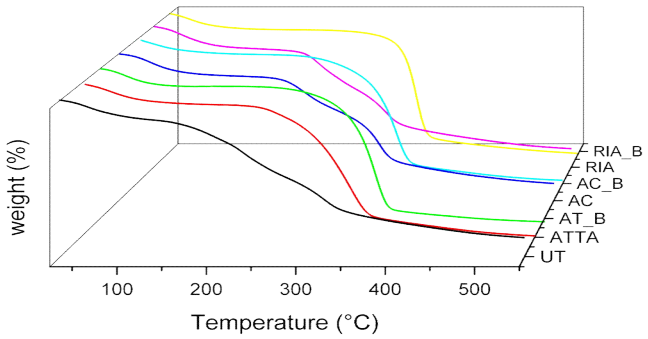

369

370 ***Fig. 4*** *TG for OB fiber and the respective treatments*

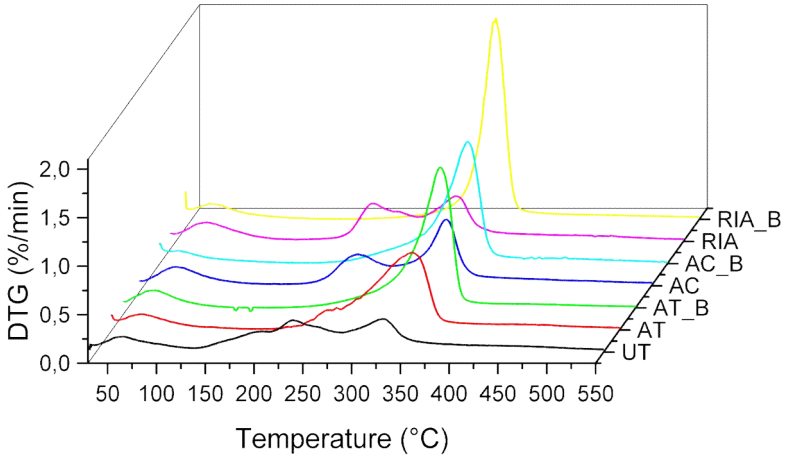

371

372 ***Fig.5*** *DTG for OB fiber and the respective treatments*

373

374 In general, the fibers is composed of hemicellulose, which degrades between 200-350°C or over
375 lower, depending on the experimental conditionals [49–52], lignin with an extensive range of degradation
376 temperature (140-800°C) [53, 54], the cellulose that presents a high thermal resistance and usually
377 degrades in the range of 300-400°C (Yang et al. 2007; Prado and Spinacé 2019; Dai et al. 2020) and some
378 impurities such as ash, extractives, waxes, and inorganic compounds that degrades in the range of 140-
379 800°C [59]. After different chemical treatments that are usually applied in the lignocellulosic fibers with

the objective of remove amorphous components, such as waxes, extractives, lignin, pectin, and hemicellulose, the number of degradation stages decreases since a more homogeneous chemical composition is reached and the perceptual amount of cellulose in the fibers increases, as shown in previous sections.

Untreated fibers presented three stages of degradation, while bleached fibers (AT_B, AIR_B, and AC_B) only two stages, indicating that a more homogeneous chemical composition was reached with the chemical treatments applied. Among AT, AC, and AIR fibers, the first presents a more homogeneous degradation with a shoulder between 150 and 300 °C due to hemicellulose degradation and a narrower peak of cellulose degradation. For AC and AIR samples, the presence of three prominent peaks is an indication that chemical treatments are less efficient in the removal of amorphous components resulting in a material with a more heterogeneous chemical composition. The alkaline treatment causes fiber expansion, increasing the pore size and accessible surface area [60].

On the other hand, during the acetosolv treatment, used to remove mainly lignin, the organic solvents provide the cleavage of the ether bonds of lignin, and also, the oxidation could be occurred due to the presence of hydrochloric acid as a catalyst reagent [61]. Finally, AIR treatment is a milder treatment that removes only the alcohol-soluble constituents such as low molecular weight and traces of free galacturonic acid [62]. For all samples, the first stage of degradation is due to the evaporation of adsorbed and absorbed water, as observed in the work of [55] and [61]. The second one is due to the degradation of hemicellulose [52], and the third one is due to cellulose degradation [63] (Fulano et al., 2001). The main degradation steps are presented in Table 5.

The weight loss of each degradation stage can be related to the effect of chemical treatment on removing specific components. The removal of each component gives particular TG curves. Ornaghi Jr et al. [64] studied the thermal decomposition of biomass using an F-test model-fitting method and confirmed the existence of three different degradation stages with a unique average activation energy value.

Tab.5 *In natura fiber (UT), AT, AT_B, AIR, AIR_B, AC and AC_B with the respectively, and the main mass loss stages*

Samples	ΔT (°C)	Tpeak (°C)	Weight loss (%)	Ti (°C)	Residue at 550°C
In natura	30-130	57	10.22	124.27	29.73
	130-280	231	29.37		
	280-360	324	18.86		
AT	30-170	60	10.63	133.45	20.68
	170-400	338	61.64		
AT_B	30-140	56	9.15	227.85	18.29
	194-404	350	67.85		
AIR	30-160	62	12.39	93.19	30.53
	160-279	232	22.95		
	279-360	318	22.96		
AIR_B	30-130	50	8.39	237.07	18.82
	245-390	342	64.45		
AC	30-165	62	11.75	103.52	29.40
	165-286	250	18.37		
	286-390	340	31.34		
AC _B	30-166	48	8.03	243.76	21.86
	190-400	345	63.69		

4. Conclusions

In this study, the importance of utilizing orange bagasse by different chemical pretreatments is demonstrated. A complete chemical structure characterization and discussion are performed, with the advantage of the proper choice of the route, depending on the interest final material. Quantification of the non-cellulosic composites is done after each pretreatment and subsequent bleaching process using FTIR, XRD, chemical composition, and TGA. Higher differences are observed in the crystallinity index and onset degradation curve (shift to higher values), mainly compared to the pretreatment used (alkaline have the best efficiency compared to organosolv and alcohol insoluble residue). All beaching process performed after each pretreatment show similar results concerning the techniques analyzed. Moreover, the pretreatments sequence is an essential factor in selecting the adequate chemical method to ensure the most efficient removal of the non-cellulosic materials.

Acknowledgment

The authors gratefully acknowledge the financial support of São Paulo Research Foundation-FAPESP (Grant n° 2015/10386-9; Grant n° 2017/19530-0, and Grant n°2016/16168-6)

References

1. Roussos PA (2016) Orange (Citrus sinensis (L .) Osbeck). Elsevier Inc.
2. Ashok B, Nanthagopal K, Perumal DA, et al (2019) An investigation on CRDi engine characteristic using renewable orange-peel oil. Energy Convers Manag 180:1026–1038. https://doi.org/10.1016/j.enconman.2018.11.047
3. López-Linares JC, Ballesteros I, Tourán J, et al (2015) Optimization of uncatalyzed steam explosion pretreatment of rapeseed straw for biofuel production. Bioresour Technol 190:97–105. https://doi.org/10.1016/j.biortech.2015.04.066
4. Romero-Lopez MR, Osorio-Diaz P, Bello-Perez LA, et al (2011) Fiber concentrate from orange (Citrus sinensis L.) bagase: Characterization and application as bakery product ingredient. Int J Mol Sci 12:2174–2186. https://doi.org/10.3390/ijms12042174
5. Cypriano DZ, da Silva LL, Tasic L (2018) High value-added products from the orange juice industry waste. Waste Manag 79:71–78. https://doi.org/10.1016/j.wasman.2018.07.028
6. Jabbar A, Militký J, Wiener J, et al (2017) Nanocellulose coated woven jute/green epoxy composites: Characterization of mechanical and dynamic mechanical behavior. Compos Struct 161:340–349. https://doi.org/10.1016/j.compstruct.2016.11.062
7. Awan AT, Tsukamoto J, Tasic L (2013) Orange waste as a biomass for 2G-ethanol production using low cost enzymes and co-culture fermentation. RSC Adv 3:25071–25078. https://doi.org/10.1039/c3ra43722a
8. Kumari D, Singh R (2018) Pretreatment of lignocellulosic wastes for biofuel production: A critical review. Renew Sustain Energy Rev 90:877–891. https://doi.org/10.1016/j.rser.2018.03.111
9. Hassan SS, Williams GA, Jaiswal AK (2018) Emerging technologies for the pretreatment of lignocellulosic biomass. Bioresour Technol 262:310–318. https://doi.org/10.1016/j.biortech.2018.04.099
10. Shimizu FL, Monteiro PQ, Ghiraldi PHC, et al (2018) Acid, alkali and peroxide pretreatments increase the cellulose accessibility and glucose yield of banana pseudostem. Ind Crops Prod 115:62–68. https://doi.org/10.1016/j.indcrop.2018.02.024
11. Lorenci Woiciechowski A, Dalmas Neto CJ, Porto de Souza Vandenberghe L, et al (2020) Lignocellulosic biomass: Acid and alkaline pretreatments and their effects on biomass recalcitrance – Conventional processing and recent advances. Bioresour Technol 304:122848. https://doi.org/10.1016/j.biortech.2020.122848
12. Balea A, Merayo N, De La Fuente E, et al (2017) Assessing the influence of refining, bleaching and TEMPO-mediated oxidation on the production of more sustainable cellulose nanofibers and their application as paper additives. Ind Crops Prod 97:374–387. https://doi.org/10.1016/j.indcrop.2016.12.050
13. Currie HA, Perry CC (2007) Silica in plants: Biological, biochemical and chemical studies. Ann Bot 100:1383–1389. https://doi.org/10.1093/aob/mcm247
14. Ferreira JA, Taherzadeh MJ (2020) Improving the economy of lignocellulose-based biorefineries with organosolv pretreatment. Bioresour Technol 299:122695.

https://doi.org/10.1016/j.biortech.2019.122695
15. Zhang K, Pei Z, Wang D (2016) Organic solvent pretreatment of lignocellulosic biomass for biofuels and biochemicals: A review. Bioresour Technol 199:21–33. https://doi.org/10.1016/j.biortech.2015.08.102
16. Waldron KW, Selvendran RR (1990) Composition of the cell walls of different asparagus (Asparagus officinalis) tissues. Physiol Plant 80:568–575. https://doi.org/10.1111/j.1399-3054.1990.tb05680.x
17. Pettolino FA, Walsh C, Fincher GB, Bacic A (2012) Determining the polysaccharide composition of plant cell walls. Nat Protoc 7:1590–1607. https://doi.org/10.1038/nprot.2012.081
18. Kabir MM, Wang H, Lau KT, Cardona F (2013) Effects of chemical treatments on hemp fibre structure. Appl Surf Sci 276:13–23. https://doi.org/10.1016/j.apsusc.2013.02.086
19. Jebali Z, Nabili A, Majdoub H, Boufi S (2018) International Journal of Biological Macromolecules Cellulose nanofibrils (CNFs) from Ammophila arenaria , a natural and a fast growing grass plant. Int J Biol Macromol 107:530–536. https://doi.org/10.1016/j.ijbiomac.2017.09.024
20. Júnior ADNF, Etchelet MI, Braga AFM, et al (2020) Alkaline pretreatment of yerba mate (Ilex paraguariensis) waste for unlocking low-cost cellulosic biofuel. Fuel 266:117068. https://doi.org/10.1016/j.fuel.2020.117068
21. Benar P, Gonçalves AR, Mandelli D, Schuchardt U (1999) Eucalyptus organosolv lignins: Study of the hydroxymethylation and use in resols. Bioresour Technol 68:11–16. https://doi.org/10.1016/S0960-8524(98)00076-5
22. Sluiter A, Hames B, Ruiz R, et al (2012) Determination of Structural Carbohydrates and Lignin in Biomass. 2011
23. Dence CW (1992) The Determination of Lignin. In: Lin SY, Dence CW (eds) Methods in Lignin Chemistry. Springer Berlin Heidelberg, Berlin, pp 33–61
24. Fan M, Dai D, Huang B (2012) Fourier Transform Infrared Spectroscopy for Natural Fibres. Fourier Transform - Mater Anal. https://doi.org/10.5772/35482
25. Pereira PHF, De Freitas Rosa M, Cioffi MOH, et al (2015) Vegetal fibers in polymeric composites: A review. Polimeros 25:. https://doi.org/10.1590/0104-1428.1722
26. Munajad A, Subroto C, Suwarno (2018) Fourier transform infrared (FTIR) spectroscopy analysis of transformer paper in mineral oil-paper composite insulation under accelerated thermal aging. Energies 11:. https://doi.org/10.3390/en11020364
27. Traoré M, Kaal J, Martínez Cortizas A (2016) Application of FTIR spectroscopy to the characterization of archeological wood. Spectrochim Acta - Part A Mol Biomol Spectrosc 153:63–70. https://doi.org/10.1016/j.saa.2015.07.108
28. Popescu CM, Singurel G, Popescu MC, et al (2009) Vibrational spectroscopy and X-ray diffraction methods to establish the differences between hardwood and softwood. Carbohydr Polym 77:851–857. https://doi.org/10.1016/j.carbpol.2009.03.011
29. Faix O (1991) Classification of Lignins from Different Botanical Origins by FT-IR Spectroscopy. Holzforschung 45:21–28. https://doi.org/10.1515/hfsg.1991.45.s1.21

30. Popescu MC, Popescu CM, Lisa G, Sakata Y (2011) Evaluation of morphological and chemical aspects of different wood species by spectroscopy and thermal methods. J Mol Struct 988:65–72. https://doi.org/10.1016/j.molstruc.2010.12.004
31. Wada M, Kondo T, Okano T (2003) Thermally induced crystal transformation from cellulose Iα to Iβ. Polym J 35:155–159. https://doi.org/10.1295/polymj.35.155
32. Cintrón MS, Hinchliffe DJ (2015) FT-IR examination of the development of secondary cell wall in cotton fibers. Fibers 3:30–40. https://doi.org/10.3390/fib3010030
33. Mariño MA, Rezende CA, Tasic L (2018) A multistep mild process for preparation of nanocellulose from orange bagasse. Cellulose 25:5739–5750. https://doi.org/10.1007/s10570-018-1977-y
34. Mariño MA, Rezende CA, Tasic L (2018) A multistep mild process for preparation of nanocellulose from orange bagasse. Cellulose 25:5739–5750. https://doi.org/10.1007/s10570-018-1977-y
35. Faix O (1988) Practical uses of FTIR spectroscopy in wood science and technology. Mikrochim Acta 94:21–25. https://doi.org/10.1007/BF01205830
36. Challinor JM (1995) Characterisation of wood by pyrolysis derivatisation-gas chromatography/mass spectrometry. J Anal Appl Pyrolysis 35:93–107. https://doi.org/10.1016/0165-2370(95)00903-R
37. Colom X, Carrillo F, Nogués F, Garriga P (2003) Structural analysis of photodegraded wood by means of FTIR spectroscopy. Polym Degrad Stab 80:543–549. https://doi.org/10.1016/S0141-3910(03)00051-X
38. Nishiyama Y, Langan P, Chanzy H (2002) Crystal structure and hydrogen-bonding system in cellulose Iβ from synchrotron X-ray and neutron fiber diffraction. J Am Chem Soc 124:9074–9082. https://doi.org/10.1021/ja0257319
39. Schwanninger M, Rodrigues JC, Pereira H, Hinterstoisser B (2004) Effects of short-time vibratory ball milling on the shape of FT-IR spectra of wood and cellulose. Vib Spectrosc 36:23–40. https://doi.org/10.1016/j.vibspec.2004.02.003
40. O'connor RT, Dupré EF, Mitcham D (1958) Applications of Infrared Absorption Spectroscopy to Investigations of Cotton and Modified Cottons:Part I: Physical and Crystalline Modifications and Oxidation. Text Res J 28:382–392. https://doi.org/10.1177/004051755802800503
41. Oh SY, Yoo D Il, Shin Y, Seo G (2005) FTIR analysis of cellulose treated with sodium hydroxide and carbon dioxide. Carbohydr Res 340:417–428. https://doi.org/10.1016/j.carres.2004.11.027
42. Carrillo I, Mendonça RT, Ago M, Rojas OJ (2018) Comparative study of cellulosic components isolated from different Eucalyptus species. Cellulose 25:1011–1029. https://doi.org/10.1007/s10570-018-1653-2
43. Mwaikambo LY, Ansell MP (2002) Chemical modification of hemp, sisal, jute, and kapok fibers by alkalization. J Appl Polym Sci 84:2222–2234. https://doi.org/10.1002/app.10460
44. Mansikkamäki P, Lahtinen M, Rissanen K (2007) The conversion from cellulose I to cellulose II in NaOH mercerization performed in alcohol-water systems: An X-ray powder diffraction study. Carbohydr Polym 68:35–43. https://doi.org/10.1016/j.carbpol.2006.07.010

45. Mansikkamäki P, Lahtinen M, Rissanen K (2005) Structural changes of cellulose crystallites induced by mercerisation in different solvent systems; determined by powder X-ray diffraction method. Cellulose 12:233–242. https://doi.org/10.1007/s10570-004-3132-1
46. Agarwal UP, Ralph SA, Reiner RS, Baez C (2016) Probing crystallinity of never-dried wood cellulose with Raman spectroscopy. Cellulose 23:125–144. https://doi.org/10.1007/s10570-015-0788-7
47. Nam S, French AD, Condon BD, Concha M (2016) Segal crystallinity index revisited by the simulation of X-ray diffraction patterns of cotton cellulose Iβ and cellulose II. Carbohydr Polym 135:1–9. https://doi.org/10.1016/j.carbpol.2015.08.035
48. Duchemin B, Thuault A, Vicente A, et al (2012) Ultrastructure of cellulose crystallites in flax textile fibres. Cellulose 19:1837–1854. https://doi.org/10.1007/s10570-012-9786-1
49. Shen D, Zhang L, Xue J, et al (2015) Thermal degradation of xylan-based hemicellulose under oxidative atmosphere. Carbohydr Polym 127:363–371. https://doi.org/10.1016/j.carbpol.2015.03.067
50. Ravindran L, Sreekala MS, Thomas S (2019) Novel processing parameters for the extraction of cellulose nanofibres (CNF) from environmentally benign pineapple leaf fibres (PALF): Structure-property relationships. Int J Biol Macromol 131:858–870. https://doi.org/10.1016/j.ijbiomac.2019.03.134
51. Ahuja D, Kaushik A, Singh M (2018) Simultaneous extraction of lignin and cellulose nanofibrils from waste jute bags using one pot pre-treatment. Int J Biol Macromol 107:1294–1301. https://doi.org/10.1016/j.ijbiomac.2017.09.107
52. Li HY, Chen X, Li YJ, et al (2018) The effect of ionic liquids pretreatment on the distribution and structure of alkali-soluble hemicelluloses from Eucalyptus. Sep Purif Technol 191:364–369. https://doi.org/10.1016/j.seppur.2017.08.058
53. Stefanidis SD, Kalogiannis KG, Iliopoulou EF, et al (2014) A study of lignocellulosic biomass pyrolysis via the pyrolysis of cellulose, hemicellulose and lignin. J Anal Appl Pyrolysis 105:143–150. https://doi.org/10.1016/j.jaap.2013.10.013
54. Galano A, Aburto J, Sadhukhan J, Torres-García E (2017) A combined theoretical-experimental investigation on the mechanism of lignin pyrolysis: Role of heating rates and residence times. J Anal Appl Pyrolysis 128:208–216. https://doi.org/10.1016/j.jaap.2017.10.009
55. Dai H, Huang Y, Zhang H, et al (2020) Direct fabrication of hierarchically processed pineapple peel hydrogels for efficient Congo red adsorption. Carbohydr Polym 230:115599. https://doi.org/10.1016/j.carbpol.2019.115599
56. Yang H, Yan R, Chen H, et al (2007) Characteristics of hemicellulose, cellulose and lignin pyrolysis. Fuel 86:1781–1788. https://doi.org/10.1016/j.fuel.2006.12.013
57. Pereira PHF, Souza NF, Ornaghi HL, de Freitas MR (2020) Comparative analysis of different chlorine-free extraction on oil palm mesocarp fiber. Ind Crops Prod 150:. https://doi.org/10.1016/j.indcrop.2020.112305
58. Prado KS, Spinacé MAS (2019) Isolation and characterization of cellulose nanocrystals from pineapple crown waste and their potential uses. Int J Biol Macromol 122:410–416.

https://doi.org/10.1016/j.ijbiomac.2018.10.187
59. Vassilev S V., Baxter D, Andersen LK, Vassileva CG (2010) An overview of the chemical composition of biomass. Fuel 89:913–933. https://doi.org/10.1016/j.fuel.2009.10.022
60. Monlau F, Kaparaju P, Trably E, et al (2015) Alkaline pretreatment to enhance one-stage CH4and two-stage H2/CH4production from sunflower stalks: Mass, energy and economical balances. Chem Eng J 260:377–385. https://doi.org/10.1016/j.cej.2014.08.108
61. Souza NF, Pinheiro JA, Brígida AIS, et al (2016) Fibrous residues of palm oil as a source of green chemical building blocks. Ind Crops Prod 94:. https://doi.org/10.1016/j.indcrop.2016.09.012
62. Oliveira TÍS, Rosa MF, Cavalcante FL, et al (2016) Optimization of pectin extraction from banana peels with citric acid by using response surface methodology. Food Chem 198:113–118. https://doi.org/10.1016/j.foodchem.2015.08.080
63. Meng F, Zhang X, Yu W, Zhang Y (2019) Kinetic analysis of cellulose extraction from banana pseudo-stem by liquefaction in polyhydric alcohols. Ind Crops Prod 137:377–385. https://doi.org/10.1016/j.indcrop.2019.05.025
64. Ornaghi HL, Ornaghi FG, de Carvalho Benini KCC, Bianchi O (2019) A comprehensive kinetic simulation of different types of plant fibers: autocatalytic degradation mechanism. Cellulose 0123456789:7145–7157. https://doi.org/10.1007/s10570-019-02610-x

Supplementary Files

This is a list of supplementary files associated with this preprint. Click to download.

- graphicabstract.jpg